LAWRENCE
LIVERMORE
NATIONAL
LABORATORY

LLNL-TR-410898

Development of Single Cell Raman Spectroscopy for Cancer Screening and Therapy Monitoring

J. W. Chan

February 27, 2009

Disclaimer

This work performed under the auspices of the U.S. Department of Energy by Lawrence Livermore National Laboratory under Contract DE-AC52-07NA27344.

FY08 LDRD Final Report
Development of Single Cell Raman Spectroscopy for Cancer Screening and Therapy Monitoring
LDRD Project Tracking Code: 06-ERD-051
James W. Chan, Principal Investigator

Abstract

The overall goal of this project was to develop a new technology for cancer detection based on single cell laser tweezers Raman spectroscopy (LTRS). This method has the potential to improve the detection of cancer characteristics in single cells by acquiring cellular *spectral markers* that reflect the intrinsic biology of the cell. These *spectral biomarkers* are a new form of molecular signatures in the field of cancer research that may hold promise in accurately identifying and diagnosing cancer and measuring patient response to treatment. The primary objectives of this proposed work were to perform a full characterization of the Raman spectra of single normal, transformed, and cancer cells to identify cancer spectral signatures, validate the clinical significance of these results by direct correlation to established clinical parameters for assessing cancer, and to develop the optical technology needed for efficient sampling and analysis of cells needed for the practical use of such a system in the clinic. The results indicated that normal T and B lymphocytes could be distinguished from their neoplastic cultured cells and leukemia patient cells with classification sensitivities and specificities routinely exceeding 90% based on multivariate statistical analysis and leave-one-out cross validation. Differences primarily in the Raman peaks associated with DNA and protein were observed between normal and leukemic cells and were consistent for both the cultured and primary cells. Differences between normal and leukemia patient cells were more subtle than between normal and leukemia cultured cells but were still significant to allow for accurate discrimination. Furthermore, it is revealed that the spectral differences are representative of the neoplastic phenotype of the cells and not a reflection of the different metabolic states (resting versus active) of normal and leukemic cells. The effect of different standard cell fixation protocols (i.e. methanol, paraformaledhye) on the Raman spectra and ultimately the ability to discriminate between cell types was also studied. Results suggest that paraformaldehyde fixation does not significantly affect the Raman signals, but methanol fixation causes inaccurate Raman classification. Development of a new optofluidic platform for analyzing and sorting cells based on Raman spectroscopy ('Raman activated cell sorting or RACS') was achieved, which lays the foundation for developing next generation Raman flow cytometry.

Introduction/Background

Current technologies for cancer detection and diagnosis typically rely on a combination of methods, such as optical microscopy, histopathology, and fluorescence flow cytometry. Some of these methods are unavoidably slow and laborious, resulting in delays in the diagnosis. They can also be invasive and destructive, leading to perturbation of the sample biology and possibly affecting the disease progression. Still others lack the sensitivity or the precise signatures of

cancer for accurate, early detection. Methods for improved detection and diagnosis of cancer that can provide new and more accurate molecular markers of cancer are desirable for positive cancer identification, leading to improved cancer treatment and therapy monitoring. Laser-based spectroscopic techniques offer a noninvasive approach to analyze live cells with near real-time results. For example, fluorescence spectroscopy has been used to discriminate between normal and neoplastic tissue[1], but often provides insufficient chemical information[2]. Raman spectroscopy is an attractive technique for cancer detection because it probes molecular bonds, yielding specific information on biochemical composition and biomolecular structural conformations and interactions[3]. Application of Raman spectroscopy to cancer detection provides potentially new and unique cancer *spectral markers* that reflect the biology of the cell, in lieu of the more common biomarkers in current cancer screening assays. The simultaneous acquisition of multiple spectral markers offers potentially more discriminating power for cancer diagnosis than testing for a single cancer biomarker. Analysis of cancer tissue using Raman spectroscopy has gradually become an established technique that has even made its way into the operating room[4], but its application to the single cell level has not yet been realized. The use of laser tweezers Raman spectroscopy for cancer detection provides an objective, quantitative, and noninvasive approach to cancer detection and diagnosis at the single cell level to detect rare events and single cell dynamics, and has the potential for immediate clinical applications as a live cell sorting technique analogous to flow cytometry. To achieve this, more studies are needed to evaluate the discriminating power and biology associated with the Raman signatures of different cellular systems.

Raman spectropy generates a "biomolecular fingerprint" of a cell based on the interaction of laser photons and molecular bonds

Raman spectroscopy is a laser-based spectroscopic technique for the analysis of molecular bonds. Raman scattering is the interaction of photons with molecular vibrations, in which a small fraction ($\sim$ 1 in 10^8 photons) are inelastically scattered and lose a portion of their energy to the molecular vibration. The difference in energy between the incident and scattered photon corresponds to the energy of the molecular vibration. Detection of these scattered photons yields a spectrum of Raman peaks, each of which can be assigned to specific molecular vibrations. Each Raman peak of a particular molecular vibration is located at a specific wavenumber shift (in cm^{-1}) from the excitation source. Therefore, a Raman spectrum functions as a "molecular fingerprint" of the sample, providing a wealth of information on the chemical bonds associated with DNA, RNA, proteins, lipids, and other biomoleules present in a cell. In addition, since a molecular vibration is sensitive to its neighboring molecular bonds and structure, Raman spectroscopy can also provide information about biomolecular conformations and intermolecular interactions. When combined with confocal microscopy, single cell and subcellular chemical information can be obtained[5].

Unlike fluorescence spectroscopy, which requires the use of exogenous labels, Raman spectroscopy is a *noninvasive* approach to acquire biochemical information from biological samples, leaving the cell intact and undisturbed. The Raman signals are intrinsic signatures of the biochemical makeup of the sample; therefore, exogenous labeling, which may alter cell biology or require cells to be fixed, is not necessary. In addition, since Raman scattering is not a real absorption process, any laser wavelength excitation can be chosen to generate a Raman spectrum. This opens up possibilities of utilizing near-infrared wavelengths to probe live biological samples, reducing the potential for laser damaging the sample and generating less autofluorescene that can interfere with the Raman signals[6]. Another advantage of

Raman spectroscopy is that the Raman signal is constant and does not photobleach, which allows long term chemical analysis of a single living cell to be performed.

Raman spectroscopy has found extensive use in biology and biochemistry for the characterization of the structure of biological molecules[7-9]. Several Raman signatures can be assigned directly to various biomolecular structures. For example, many amino acids, such as tyrosine, tryptophan, and phenylalanine, have distinct peaks in the 600 to 1700 cm^{-1} fingerprint region. Amide linkages between amino acids give rise to two Raman active vibrations, the amide I C=O stretch mode, and the amide III C-N stretch and N-H in-plane bending modes. The relative positions of these two vibrations can give information about whether the secondary structure of the proteins are in alpha helical or beta sheet conformations. DNA has several distinct spectral peaks that can either be assigned to the sugar phosphate backbone or to the four DNA bases. The symmetric stretching of two phosphate oxygens in the diphosphate ester PO^{2-} group occurs at 1100 to 1150 cm^{-1}. The O-P-O assymetric strecth of DNA is situated at 835 cm^{-1}, and the O-P-O stretch between nucleotides for DNA and RNA occurs at 800-815 cm^{-1}. The exact positions of these peaks can provide information on the DNA conformation (A, B, C, Z) or subtle changes to the DNA structure. Phospholipid molecules, which make up cellular membranes, have spectral markers due to both the head and tail[9]. For example, polar head groups have a C-N stretch at 720 cm^{-1}, while hydrophobic chains have vibrational peaks in the 1000-1150 cm^{-1} region due to C-C skeletal modes. The intensity and location of these peaks are extremely sensitive to the structural conformation of the chains and therefore, varies depending on whether they are trans or gauche configurations, and saturated or unsaturated chains. *Cis* and *trans* structures of the C=C group can be elucidated by identification of lipid related peaks at 1655 and 1668 cm^{-1} respectively.

Raman detection and classification of cancer in tissues and bulk cells

Since it is known that the onset of neoplasia is accompanied by abnormal cellular composition and distribution, molecular conformations, and metabolic activity, Raman spectroscopy has the potential to detect such changes spectroscopically in-vivo and in-vitro. Over the past ten years, many studies have demonstrated the application of Raman spectroscopy to the study and diagnosis of cancer disease[10-27]. These studies have used Raman spectroscopy to detect cancers primarily in tissues and bulk cell populations from e.g. the breast, brain, colon, bladder, lung, and cervix. The spectral signatures can then be used to classify normal and cancer samples and also determine the progression of the disease stage. For example, a study by Haka et. al.[11] used Raman spectroscopy to differentiate benign and malignant lesions in human breast tissue and were able to use the ratio of spectroscopic signatures specific to collagen, fat, and nuclear to cellular cytoplasm to classify the samples according to their pathological diagnosis with high sensitivity. Min et. al.[28] has been able to detect differences in select bands associated with amide I protein (1670 cm^{-1}) and CH_2 bending vibrations at 1450, 1490, and 1449 cm^{-1} to discriminate between normal, adenocarcinoma, squamous cell carcinoma human lung tissue. Nijssen et. al.[22] discriminated basal cell carcinoma regions from noncancerous surrounding tissue utilizing a combination of Raman spectroscopy and Raman imaging (imaging tissue based on location of the spectral markers). A combination of 14 different spectral components ranging from 727 to 1651 cm^{-1} that were assignable to DNA, RNA, lipid, amide and amino acid structures, were found for normal and neoplastic tissues. Utzinger et. al.[23] studied squamous dysplasia (cervical precancer) and delineated high-grade dysplasia from all others based on observed alterations in peaks assigned to collagen, phospholipids, and DNA.

With real-time, objective diagnosis of pathologies the ideal standard for cancer diagnosis, the use of spectral results from Raman spectroscopy and

subsequent statistical analysis offers great potential for automated diagnostic routines. The spectral differences can be used in diagnostic algorithms to enhance the differentiating ability, improve classification, and provide automated, clinical diagnosis. The simplest of routines is by looking at variations in peak intensities, peak positions, and relative peak ratios. Often, however, multiple markers may contribute to the differences between two types of cancer or a normal and a cancer tissue. In essence, the attractiveness of the spectral results is to be able to use multiple markers for more discriminating power. In addition, the majority of the spectral features do not contribute significantly to the discrimination process. Therefore, more elaborate multivariate statistical techniques are being used[29-31], such as PCA, LDA, and hierarchical clustering, for a combination of data reduction to identify the most important variables and improve data classification. The use of these methods also provides a clearer presentation of the data in the form of a scatter plot for easier visualization of data groups.

Laser tweezers Raman spectroscopy offers rapid approach to single cell analysis in suspension

Although Raman spectroscopy has become a fairly mature technology, its development and application for *single cell* cancer detection has, to date, been largely lacking. A comprehensive survey of the 'Raman-cancer' work, to date, shows that the majority has focused instead on in-vivo detection applications at the more *macroscopic tissue* level, as discussed above. Single cell detection, in particular when dealing with samples at extremely low cell concentrations, poses several technical challenges that must be addressed by a combination of optical technology development and adaptation of the Raman technique to specific applications.

Raman spectroscopy of individual cells, and in particular single suspension cells in solution, is often laborious and time consuming, requiring the cell to be immobilized on a surface prior to its spectral analysis. Otherwise, suspension cells would float in and out of the laser beam and acquiring its Raman spectrum would be impossible, since acquisition times are typically 1 to 2 minutes. Surface adhesion may possibly modify the biological properties of the cell, and the Raman signals from the surface substrate can interfere with the desired Raman spectra of the cell. The use of laser tweezers Raman spectroscopy (LTRS) for single cell analysis overcomes these issues and provides a method to rapidly acquire the spectral fingerprint of single cells.

The technique of laser tweezers (i.e. optical trapping), first demonstrated by Ashkin et. al. with a single laser beam trap[32], has found many biological applications such as the physical manipulation of single cells and organelles[33,34] and studies involving protein motor forces[35,36]. Optical trapping in its simplest form involves the use of a single, tightly focused Gaussian shaped laser beam to optically trap and immobilize a cell, or subcellular component, within the laser focus in solution. The trapping phenomenon is achieved as photons impinging on the particle transfer momentum from the light beam to the object due to refraction and scattering of the photons, resulting in both transverse and axial forces imparted on the particle that are balanced near the laser focus[37]. This results in a stable three dimensional optical trap to hold a single cell suspended in solution away from any surfaces.

The combination of laser tweezers with micro-Raman spectroscopy (LTRS) has only recently been applied to the chemical analysis of individual living biological cells[9,38-42]. The development of powerful near-infrared diode lasers has enabled the optical trapping of biological cells with high powers without damaging the cell within the tight focus due to the low absorption of this wavelength of light by biological materials. Simultaneous Raman spectral acquisition from the cell can be achieved within minutes due to the use of such high powers. In this configuration, a single

focused laser beam functions as both the laser tweezers and the excitation source for Raman spectroscopy. Laser tweezers Raman spectroscopy is ideally suited for the analysis of single cells because by holding the particle in the focus, it also maximizes the Raman signal. Other benefits include the ability to monitor the cells over extended periods of time while not compromising the biological activity of the cells. Rapid sampling of different cells in solution is allowed by LTRS, providing a more practical method of cell analysis in a clinical environment, similar to flow cytometry. Individual cells can be probed in solution, and particle distributions of heterogeneous populations can be obtained, which is not possible with conventional bulk Raman spectroscopy. More importantly, the addition of laser tweezers to Raman spectroscopy offers the ability to physically sort cells based on their intrinsic chemical differences by laser manipulation of the cells. This sorting mechanism would allow unperturbed cells to be classified and set aside for additional analyses.

Another benefit of LTRS is that it provides a method to study the dynamic cellular processes of a single cell in near real-time as it undergoes various metabolic activities or is perturbed by external stimuli by monitoring the Raman signatures of the single cell over an extended time period. Several recent studies have demonstrated such single cell analyses. Work by Mannie et al.[42] presented the use of LTRS as a means to reveal the activation status of individual T cells by monitoring changes in Raman spectroscopic signatures associated with DNA and protein upon exposure to stimuli. Other studies have monitored the apoptotic process of individual yeast and bacterial cells upon heating the sample and observed changes in peaks associated with phenylalanine, which indicated that proteins were unfolding during the heat-denaturation process[43]. Ajito et. al.[44] used a laser trapping Raman technique to monitor the release rate and amount of glutamate in individual synaptosomes from Wister rat brain upon addition of specific chemicals acting as K+-channel blockers. A study[45] investigating the response of red blood cells upon exposure to alcohol observed RBC degradation due to the loss of hemoglobin molecules, which is reflected in a drop in the 752 cm^{-1} porphyrin ring breathing vibration associated with the heme group.

Research Activities and Results

Cell preparation methods

Human peripheral blood mononuclear cells (PBMC) were obtained by Ficoll-Hypaque density gradient of heparinized venous blood obtained from healthy volunteers and leukemia patients. The cells were washed 3 times in RPMI 1640 medium prior to purification. T-cells were separated by rosette formation with activated sheep red blood cells followed by Ficoll-Hypaque density gradient centrifugation. The lymphocytes in the B-enriched fraction are routinely greater than 95% surface immunoglobulin positive as assessed by flow cytometry. T-cells were recovered from the rosetted pellet after twice lysing the sheep red blood cells with ammonium chloride buffer and thrice washing with RPMI 1640 medium. Both T- and B-cell populations were suspended in RPMI 1640 medium supplemented with 10% fetal calf serum at a density of approximately 10^6 cells/ml. Cell preparations were >99% viable as assessed by trypan blue dye exclusion. Immediately prior to Raman spectra analysis the cells were washed and suspended in phosphate buffered saline (PBS). Raji B cells and Jurkat T cells were obtained from American Type Culture Collection (ATCC, Rockville, MD) and maintained in culture with RPMI 1640 medium supplemented with 10% fetal calf serum. The cells were also washed and suspended in phosphate buffered saline immediately prior to the Raman spectroscopic analysis. The use of fresh human samples for this study was in accordance with the University of California Institutional Review Board practice guidelines.

Spectral acquisition from individual cells

Our work[46] focused on identifying and characterizing the Raman spectral differences between normal T and B cells and transformed Jurkat T and Raji B cultured cells, which we used as our initial model system for cancer in this study. Raman spectra of individual cells are acquired using a confocal Raman microscope system consisting of a continuous wave (CW) 633 nm He-Ne laser beam delivered into an inverted optical microscope and into a 100X 1.3 NA oil immersion objective, resulting in a diffraction limited spot of roughly 1 μm diameter at the laser focus. Typical laser powers at the laser focus are 8-10 mW. The beam is focused through a glass coverslip of thickness 0.17 mm, which rests on a computer controlled nanopositioning stage capable of scanning samples over a 100 μm x 100 μm region. Cells in buffer solution placed on the coverslip are probed by the laser and spectroscopic signals generated at the focus are collected by the same objective, focused through a 100 μm pinhole for background signal rejection, and directed into a spectrometer equipped with a camera which has a 1340 x 100 pixel CCD array. An acquisition time of 2-3 minutes for each cell is sufficient to yield Raman spectra with well-defined peaks. The tightly focused laser beam enables simultaneous optical trapping of individual cells and Raman interrogation (Figure 1a). A floating cell positioned near the focus of the laser beam becomes stably trapped and immobilized in three dimensions, roughly 15 μm above the coverslip surface. Human T and B cells of roughly 6 μm diameter are easily trapped and isolated away from the substrate and other cells. Figure 1b illustrates the spectral differences between the normal B cells (black) and their neoplastic Raji B counterparts (red). The spectra are averaged over between 20-40 cells for each cell type. Also shown, for clarity, is the difference spectra, obtained by subtracting the normal cell spectra from the cancer cell spectra. Consistent spectral differences are clearly observed in both the T and B cell cases. The most obvious differences between normal cells and transformed cell lines can be found in the peaks at 678 cm^{-1}, 785 cm^{-1}, 1093 cm^{-1}, 1126 cm^{-1}, 1337 cm^{-1}, 1373 cm^{-1}, 1447 cm^{-1}, 1485 cm^{-1}, 1510 cm^{-1}, and 1575 cm^{-1}. These select peaks have significantly different ($p << 0.05$) mean intensities as determined by T-test analysis. In general, most features of the Raman spectra of normal T and B cells are very similar, but quite distinct from those of Raji and Jurkat cells, which in turn are both quite similar if compared against each other. The peaks at 678 cm^{-1}, 785 cm^{-1}, 1337cm^{-1}, 1373cm^{-1}, 1485 cm^{-1}, 1510cm^{-1}, and 1575 cm^{-1}, which are almost exclusively due to ring breathing modes of DNA bases, are significantly reduced in intensity in Jurkat and Raji spectra, indicating that the overall DNA concentration in the probe volume of the laser beam is significantly lower in transformed cells than in normal cells. This is further confirmed by the similarly reduced intensity of the 1093 cm^{-1} mode of the symmetric PO_2^- stretching vibration of the DNA backbone. Some peaks that are due to protein vibrations, however, are significantly stronger in intensity in transformed cells. This is the case for the 1126 cm^{-1} C-N stretching vibration, and the 1447 cm^{-1} CH_2 deformation mode, which indicates a higher protein concentration in transformed cells than in normal cells. Another subtle difference that distinguishes transformed cells from normal cells is the presence of slight shoulders in their spectra at 813 cm^{-1} and 1240 cm^{-1}. These are the positions of the two most distinct peaks for RNA and might indicate a slightly elevated concentration of RNA in the transformed cells versus the normal cells. In summary, our Raman spectra of individual transformed and normal cells indicate significantly lower DNA concentrations and higher protein concentrations in transformed cells with potentially higher RNA concentrations.

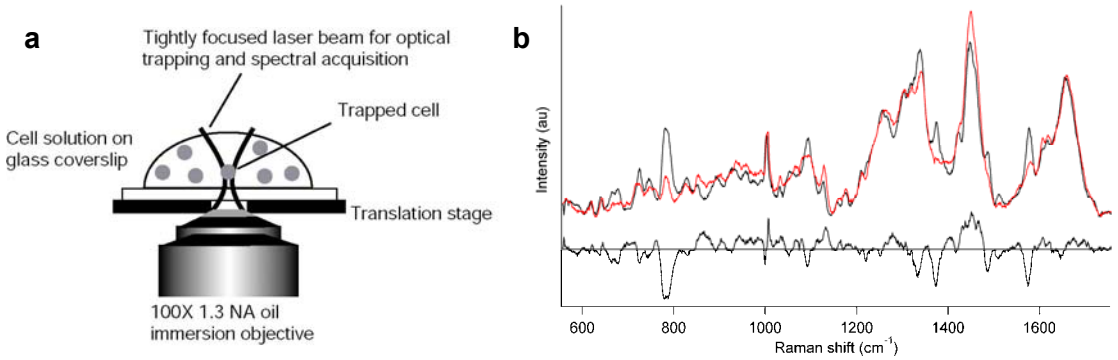

Figure 1 – (a) Illustration of the trapping of individual suspension cells in solution with a tightly focused laser beam and simultaneous Raman detection for rapid analysis and sampling of single living cancer cells. (b) Raman spectra of normal B (black) and transformed Raji B (red) cells, averaged over 20-40 cells each. Also shown below are the difference spectra that highlight the spectral differences between normal and neoplastic cells. Normal T and Jurkat T cells exhibit similar spectral differences (data not shown).

These main distinguishing spectral features between normal and transformed cells are very plausible because typical characteristics of transformed cells include increased levels of RNA, a much larger nucleus, and reduced cytoplasm. The larger nucleus in transformed cells likely affects the compactness of the chromatin and thus the concentration of DNA in the probe volume. This explains why the neoplastic cell spectra exhibit lower DNA spectral signals as a result of the lower concentration of DNA because of the larger nucleus. In addition, the decrease in DNA intensities, in particular, can be attributed to the large number of transcriptive and replicative activities occurring in these active cancer cells, which results in the decondensation of chromatin structure. The increase in proteins that we observe spectroscopically may indicate the increase in production of proteins to support the increased biomolecular synthesis.

Multivariate statistical analysis of spectral data

The experimental data analyses must be coupled with multivariate statistical methods for the purpose of extracting pertinent information and data classification. Each Raman spectrum consists of 1340 channels of data points, with only a fraction of those channels holding important spectral information (select peaks) for cell discrimination. PCA is a standard multivariate statistical technique that we have used to reduce the large amount of spectral content contained in the Raman spectra into fewer (usually two or three) important parameters (principal components). These principal components capture a specific combination of the original spectral data points such that the variance in the data structure is maximized. By utilizing PCA, we are able to perform an automated routine for analyzing and comparing individual cell spectra and eliminate the need to perform tedious statistical analysis and comparison of individual channels. A scatter plot generated from this data transformation shows clusters of points representing different cell groups, in which each point represents an individual cell. This graphical representation is similar to results obtained from flow cytometry.

Principal component analysis was performed on the individual Raman spectra. Direct comparisons between normal T and B cells and their respective transformed counterparts, Raji and Jurkat, are presented in Figures 2a and 2b. The PCA plots

show that the normal cells form distinct, separate clusters from the neoplastic cells. The sensitivity of this technique for identifying transformed cells is calculated to be 97.8%, with a Jurkat T cell specificity of 95.5%. The total number of cells correctly classified is 96.7%. PCA analysis with the two B cell groups (Figure 2a) is able to correctly classify all cell types into their respective cluster, indicating a sensitivity of 100%. Although the transformed cell lines, Jurkat and Raji, form a cluster different than the normal cells, it is not possible to positively delineate between the normal cells, or between the transformed cell lines. Sensitivity values are determined using a leave-one-out cross validation technique in combination with canonical variate analysis (CVA). In this technique, a single spectrum (i.e. blind sample) is removed from the rest of the data, which serves as the training set. The PCs derived from the training set are used as inputs to CVA to develop a classification group, which is then used to classify the single, blind spectrum. This is done repeatedly for each spectrum in the data set. Similarly, a five-fold validation method can be used, in which the data set is randomly split into five groups, and each group, in turn, is used as a blind set.

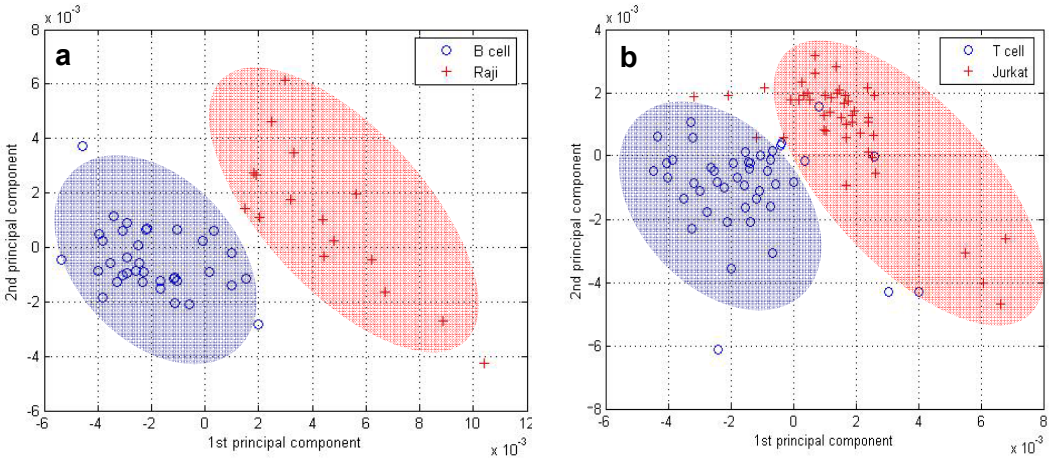

Figure 2 – PCA plots showing distinct separation of clusters according to cell type. The first two principal components are used for the 2-D scatter plot. (a) normal B cells with Raji B cells (b) normal T cells with Jurkat T cells (c) normal T cells with patient leukemia T cells.

Analysis of patient samples

Our work[47] has extended to the analysis of patient samples, where we have observed similar results. Figure 3a shows an example of the Raman differences between normal and leukemia patient cells and Figure 3b shows the clear separation in a PCA plot. These results were observed for a total of three patients, two diagnosed with B leukemia and one with T leukemia. These results are further evidence that the spectral differences are associated with cancer, and not a result of cultured cells being 'immortalized' or different due to extensive number of passages of the cell line. Furthermore, since the cell sizes of the patient and normal T cells are equivalent, the spectral differences cannot be purely associated with differences in cell size and morphology. This was a potential concern when using cultured cells, which tended to be slightly arger than the normal cells isolated from healthy individuals.

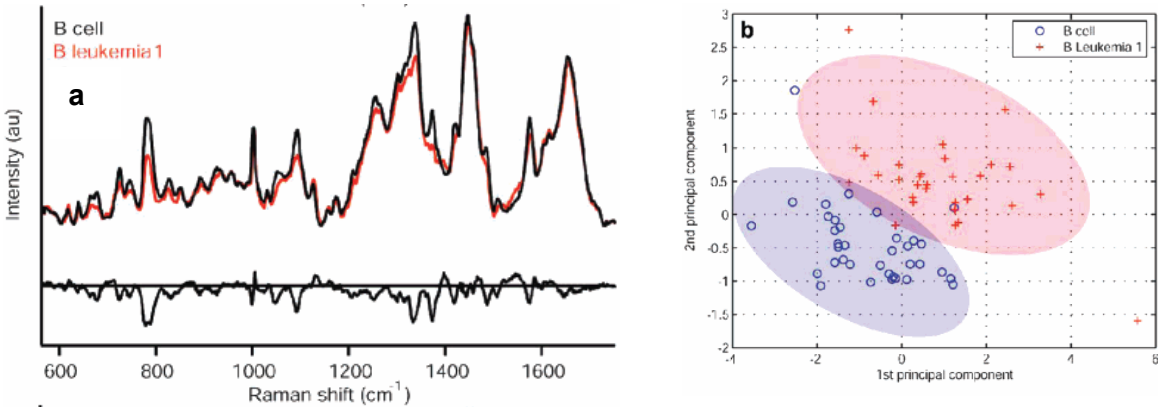

Figure 3 – (a) Averaged and difference Raman spectra of normal and patient derived leukemic B cells. Similar observations were made for 2 other patients. (b) PCA plot shows distinct separation of clusters according to cell type. The first two principal components are used for the 2-D scatter plot.

Activated cells versus non-activated cells

What is the underlying cellular biology that accounts for the spectral differences between normal and cancer cells? Are the differences simply a reflection of normal cells being in a resting phase of the cell cycle whereas leukemic cells are metabolically more active? For example, previous work[48,49] has suggested that these spectral differences are a reflection of cancerous cells being in different metabolic states than normal cells, which are predominantly in the G0 resting phase of their cell cycle. The decrease in local DNA concentration based on lower Raman intensities, in particular, has been attributed to higher levels of transcriptional and replicational activities occurring in metabolically more active cancer cells, which results in the decondensation of chromatin structure and an associated increase in proteins to support biomolecular synthesis. In addition, the morphology of cancer cells, specifically the enlarged nucleus, results in a lower DNA density in our probe volume. To evaluate this hypothesis, we compared the Raman spectra of cancer cells to those of activated normal cells using PCA to determine the degree of overlap between the two cell types. Previous Raman measurements of T cell activation[50] have shown decreases in peak intensities at 785, 1093, 1376, and 1581 cm^{-1}, which are consistent with our data on activated normal cells. The spectral changes likely reflect alterations in the secondary or tertiary structure of nucleic acids, or an unfolding of the DNA molecules as the cells become more active in their transcription, leading to a locally lower DNA concentration as it expands and requires more space. In our PCA scatter plots (see Figure 4), the cluster of activated normal cells is located in a separate region from the cancer cells and falls within the normal cell region. This suggests that the spectral differences between normal lymphocytes and leukemia cells are likely attributable to other factors that lead to more pronounced effects than just cell activation such as the faster proliferation rate of cancer cells, which results in more of the cells having heightened metabolic activity, cell growth differentiation, and transcriptional activity. Additional studies are needed to more precisely control some of these aspects and further elucidate these issues but are beyond the scope of this proposal.

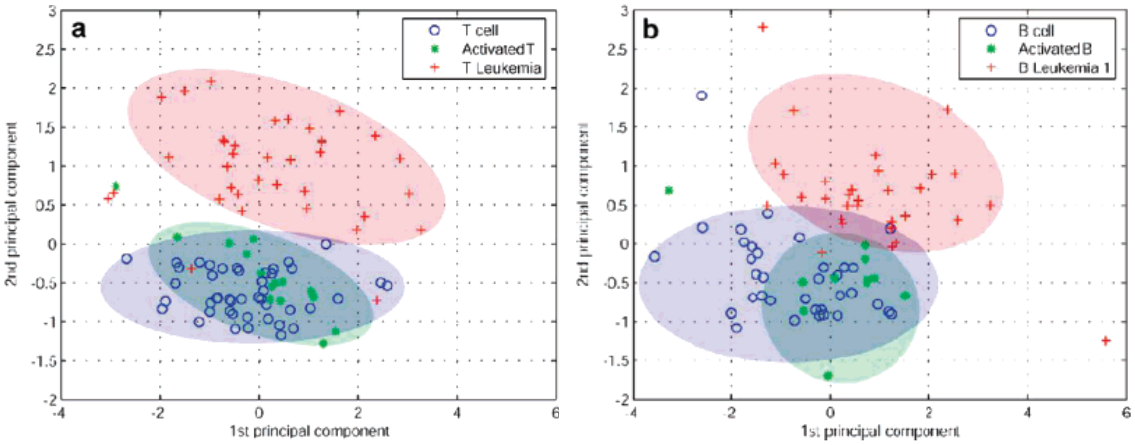

Figure 4 – PCA plots comparing normal, activated, and patient leukemic cells for (a) T lymphocytes and (b) B lymphocytes. Overlap of the intentionally activated cells and the normal resting cells indicate that the Raman differences between normal and leukemia cells are indicative of more than the phase of the cell cycle.

Cell fixation studies

Laser tweezers Raman spectroscopy (LTRS) was used to characterize the effect of different chemical fixation procedures on the Raman spectra of normal and leukemia cells[51]. This study is important because often, clinical samples that are received from pathology are already chemically treated for flow cytometry analysis. This requires a fundamental Raman study to determine the effect of these procedures on the intrinsic Raman spectra of the cells. Individual unfixed, paraformaldehyde-fixed, and methanol-fixed normal and transformed lymphocytes from three different cell lines were analyzed with LTRS. When compared to the spectra of unfixed cells, the fixed cell spectra show clear, reproducible changes in the intensity of specific Raman markers commonly assigned to DNA, RNA, protein, and lipid vibrations (e.g. 785 cm^{-1}, 1230 cm^{-1}, 1305 cm^{-1}, 1660 cm^{-1}) in mammalian cells, many of which are important markers that have been used to discriminate between normal and cancer lymphocytes. Statistical analyses of the Raman data and classification using principal component analysis (PCA) and linear discriminant analysis (LDA) indicate that methanol fixation induces a greater change in the Raman spectra than paraformaldehyde. In addition, we demonstrate that the spectral changes as a result of the fixation process have an adverse effect on the accurate Raman discrimination of the normal and cancer cells. Figure 5 shows the PCA results of three separate measurements in which Raman spectra were taken of normal and leukemic cells that were unfixed, paraformaldehyde fixed, and methanol fixed. It is clear from the scatter plot that paraformaledehyde fixation induces minimal alterations to the discrimination of normal and leukemia cells, while methanol fixation results in significiant overlap of the cancer cells into the normal cell group. The spectral artifacts created by the use of fixatives indicate that the method of cell preparation is an important parameter to consider when applying Raman spectroscopy to characterize, image, or differentiate between different fixed cell samples to avoid potential misinterpretation of the data.

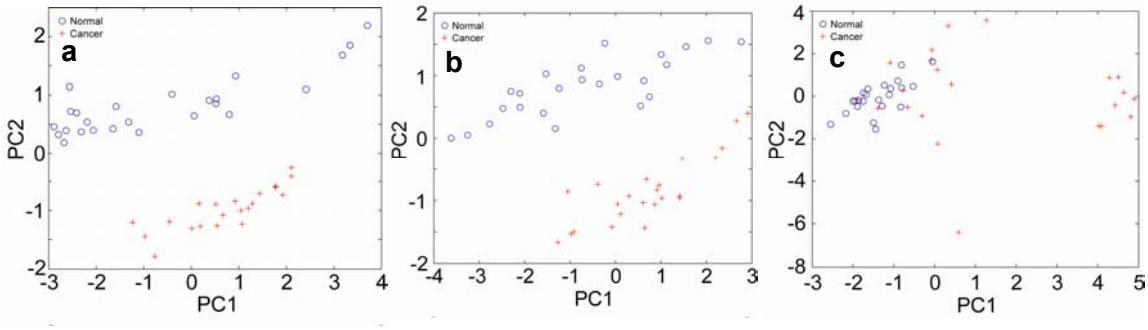

Figure 5 – PCA scatter plots comparing (a) unfixed, (b) paraformaldehyde-fixed, and (c) methanol-fixed normal and cancer cells reveal that methanol fixation leads to the greatest misclassification of cancer and normal cells.

Microfabricated devices for single cell analysis

Optofluidics refers to an emerging research field focused on implementing optics into microfluidic platforms. The combination and integration of optical and microfluidic systems intends to achieve a high level of integration, while also allowing the devices to be highly reconfigurable for the handling, manipulation, and multi-modal analysis of small quantities of biological samples. Optofluidic technologies have the potential to be developed into low-cost and compact devices for a variety of biophotonic applications.

In this study, we propose a novel use of microfluidics with LTRS for the development of a 'Raman flow cytometer'[52], an integrated optofluidic Raman activated cell sorter (RACS) for the automated delivery, manipulation, analysis, and sorting of single cells from a continuous flow of cell samples. The basic principle of RACS is not unlike that of conventional flow cytometry; both require the focusing of a stream of cells towards a laser beam for spectral analysis followed by cell sorting based on their unique spectral profile. However, one of the main reasons alternative microfluidic designs are currently needed for LTRS analysis of large cell populations is the long interrogation times required for label-free Raman analysis of an individual cell, which can range from many tens of seconds to several minutes. This requires a trapped cell to be moved from the stream of cells during the spectral acquisition so that cells flowing downstream do not knock the trapped cell out of the laser focus or also get trapped by the laser and interfere with the signal collection.

The operating principle of our proposed optofluidics RACS system is illustrated in the diagram shown in Fig. 6(a). The system consists of multiple channels. One is designated as the inlet channel for the delivery of a stream of cells into the device. Channels adjacent to the inlet channel are used as sorting channels. The laser trap is positioned on-axis in the center of the inlet channel and can be placed near the exit port of the device. The laser traps a flowing cell and pulls it to a side stream for the Raman analysis, after which the laser trap can release the cell into the adjacent sorting channels depending on its spectral signature. To sample more cells, this process is repeated continuously. An example is shown in Figure 6a of a hydrodynamic focusing device. This microfluidic design consists of a splitting channel that creates three separate laminar flow regions. The optical trap (i.e. laser focus) is positioned at the center of the channel near the exit port of the device. Cells flowing through the channel are pre-focused within a narrow center stream (i.e. inlet channel), and by default the cells all flow into the center output channel due to laminar flow. Due to the positioning of the laser trap, single cells will be trapped at the laser focus while moving along the middle stream. Once a cell is trapped, the laser is translated perpendicular to the channel length to move the cell out of the flow stream into a neighboring buffer

stream. At this time a Raman spectrum of the cell is obtained and the cell type is identified based on the spectral data. The cell is then translated to a corresponding sorting side channel and released into the flow. The laser beam is repositioned to the center of the inlet channel to trap another cell, and the process is repeated. An example of a Raman spectrum obtained from a single-cell in this manner is shown in. Note that there will be many cells that will flow out of the exit port of the device during the time that it takes to perform Raman analysis of the trapped cell. Cells from the exit port can be recollected and pumped back into the inlet port of the device to form a continuous loop. While immersed in growth media and maintained at 37 C, these recycled cells should remain viable as it continues to circulate within the system.

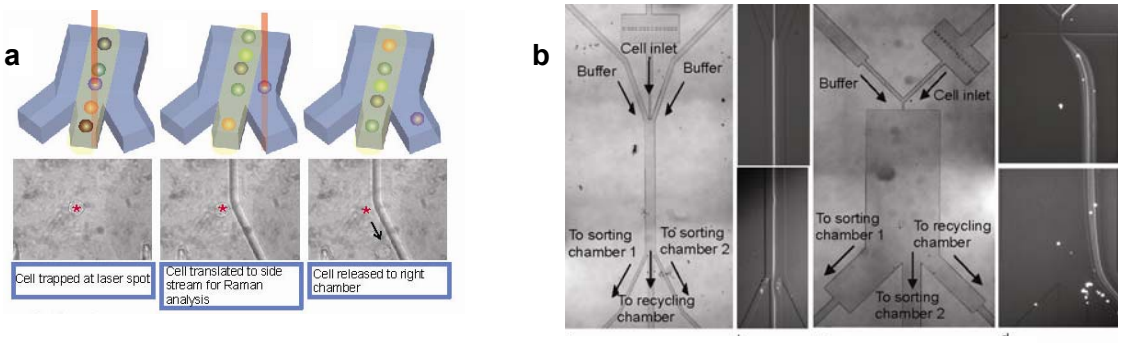

Figure 6 – (a) Illustration of the operating principles of the optofluidic RACS platform. The three major steps during the Raman analysis and sorting process, paired with image snapshots showing the trapping and sorting process of a single cell. Cells flow down the center channel, and the laser tweezers trap and move the cell into a neighboring side channel for Raman analysis. Cells are then released from the laser trap and flow downstream to their sorting channel. The laser focus spot is indicated in the inset (* marks the location of the laser focus). (b) Images of two different microfluidic devices that are evaluated in this study. White light images of the hydrodynamic focusing and pinch flow fractionation device. 5-second exposure images showing the cell flow stream at the inlet and at the outlet of the devices are also presented. HeLa cells are stained with Calcein AM dye.

Two microfluidic chip designs shown in Fig. 6b were evaluated for its suitability for implementation with LTRS for Raman sorting. The first design of the device One is based on hydrodynamic focusing of cells to the probe laser, a concept that is similar to the type used in commercial fluorescence activated cell sorting (FACS) systems. Our device consists of one central input channel and buffer inputs on both sides. The height of the channels is 50 μm and the width of the main channel is 100 μm. The square chamber at the inlet is 400 x 200 microns. The two buffer inputs hydrodynamically focus the cells into a narrow stream down the center channel. Fig. 6b also shows 5 second exposure time images of fluorescently stained cells flowing into and out of the device respectively to illustrate the flow profile. In addition to its primary function for hydrodynamic focusing, the buffer inputs also maintain the flow streams that guide the sorted cells into their corresponding output chambers. The cells flowing out of the center channel can be recollected in a recycle chamber and delivered back to the device. The fluid in the main channel can consist of standard fresh media, serum, and other nutrients that are normally used to grow and sustain the cells. However, this media is often unsuitable for Raman spectroscopy because it can yield a fluorescent background signature that interferes with the Raman signature of the cell. Moving the trapped cell to a side channel that contains a phosphate buffered saline (PBS) solution, for example, allows the cell to be washed prior to the Raman analysis, automatically reducing the fluorescence background. The second device is based on the pinch-flow fractionation concept, where its first microfluidic implementation was demonstrated by Yamada et al[53]. Cells are introduced from

the top right inlet of the device, while a second flow stream is introduced through a narrow channel at the center of the device. The flow profile of the cells is altered by the flow stream through this narrow channel and is dependent on the size of the cells. Hence, cells of a similar size follow a well-defined stream when they come out of the narrow channel. The flow stream containing the cells is directed to the right side of the channel due to the flow separation, and by default, the cells are collected downstream in the right chamber. The flow profile of fluorescently stained cells is shown. Cells can be trapped from the flow stream on the right and moved to the buffer streams on the left during the Raman analysis. Sorting channels are located downstream on the left side of the device for collection of the cells post-analysis.

Exit Plan

The project has resulted in ~5 peer-reviewed publications and numerous invited conference presentations. The results have been used to apply to several NIH grants specifically targeting the IMAT program of NCI. Several grants are pending. Also, we have spoken to several cancer foundations that are interested in pursuing this technology further. In collaboration with CBST, there is interest in starting a company based on this technology. The technology that is developed here also can be used for other applications such as detection of infectious disease and biodetection applications. Funding will be pursued through other agencies such as DoD, DHS, and DARPA.

Summary

In summary, LTRS has proven to be a powerful technique for characterizing the biochemical composition of individual, live cells without the need to add exogenous labels. As such, there is tremendous potential for developing this technique for cancer detection and to monitor therapy. This project has demonstrated the identification of leukemia cells from cultured cells and patient cells with high sensitivity and specificity. Comparable to current flow cytometry techniques, LTRS can be used to analyze and sort cells based on their intrinsic Raman signatures. In order to achieve this end, this project has focused on developing a novel optofluidic platform based on multichannel microfluidic devices for LTRS analysis and sorting. This platform can potentially lead to the next generation 'Raman activated' cell sorters.

References

1. Glasgold, R. et al. Tissue Autofluorescence as an Intermediate End-Point in Nmba-Induced Esophageal Carcinogenesis. *Cancer Letters* **82**, 33-41 (1994).
2. Kobayashi, M. et al. Detection of early gastric cancer by a real-time autofluorescence imaging system. *Cancer Letters* **165**, 155-159 (2001).
3. Baena, J. R. & Lendl, B. Raman spectroscopy in chemical bioanalysis. *Current Opinion in Chemical Biology* **8**, 534-539 (2004).
4. Haka et. al. In vivo margin assessment during partial mastectomy breast surgery using Raman Spectroscopy. Cancer Research **66**, 3317-3322 (2006)
5. Puppels, G. J. et al. Studying Single Living Cells and Chromosomes by Confocal Raman Microspectroscopy. *Nature* **347**, 301-303 (1990).
6. Puppels, G. J. et al. Laser Irradiation and Raman-Spectroscopy of Single Living Cells and Chromosomes - Sample Degradation Occurs with 514.5nm

but Not with 660nm Laser-Light. *Experimental Cell Research* **195**, 361-367 (1991).
7. Mahadevan-Jansen, A. & Richards-Kortum, R. Raman Spectroscopy for the detection of cancers and precancers. *Journal of Biomedical Optics* **1**, 31-70 (1996).
8. Peticolas, W. L. Raman-Spectroscopy of DNA and Proteins. *Biochemical Spectroscopy* **246**, 389-416 (1995).
9. Chan, J. W., Motton, D., Rutledge, J. C., Keim, N. L. & Huser, T. Raman spectroscopic analysis of biochemical changes in individual triglyceride-rich lipoproteins in the pre- and postprandial state. *Analytical Chemistry* **77**, 5870-5876 (2005).
10. Crow, P. et al. Assessment of fiberoptic near-infrared Raman spectroscopy for diagnosis of bladder and prostate cancer. *Urology* **65**, 1126-1130 (2005).
11. Haka, A. S. et al. Diagnosing breast cancer by using Raman spectroscopy. *Proceedings of the National Academy of Sciences of the United States of America* **102**, 12371-12376 (2005).
12. Huang, Z. W., Lui, H., McLean, D. I., Korbelik, M. & Zeng, H. S. Raman spectroscopy in combination with background near-infrared autofluorescence enhances the in vivo assessment of malignant tissues. *Photochemistry and Photobiology* **81**, 1219-1226 (2005).
13. Krishna, C. M. et al. Evaluation of the suitability of ex vivo handled ovarian tissues for optical diagnosis by Raman microspectroscopy. *Biopolymers* **79**, 269-276 (2005).
14. Lau, D. P. et al. Raman spectroscopy for optical diagnosis in the larynx: Preliminary findings. *Lasers in Surgery and Medicine* **37**, 192-200 (2005).
15. Yu, G. et al. Studies on human breast cancer tissues with Raman microspectroscopy. *Spectroscopy and Spectral Analysis* **24**, 1359-1362 (2004).
16. Sigurdsson, S. et al. Detection of skin cancer by classification of Raman spectra. *Ieee Transactions on Biomedical Engineering* **51**, 1784-1793 (2004).
17. Krishna, C. M. et al. Micro-Raman spectroscopy for optical pathology of oral squamous cell carcinoma. *Applied Spectroscopy* **58**, 1128-1135 (2004).
18. Crow, P., Uff, J. S., Farmer, J. A., Wright, M. P. & Stone, N. The use of Raman spectroscopy to identify and characterize transitional cell carcinoma in vitro. *BJU International* **93**, 1232-1236 (2004).
19. Huang, Z. W. et al. Near-infrared Raman spectroscopy for optical diagnosis of lung cancer. *International Journal of Cancer* **107**, 1047-1052 (2003).
20. Stone, N., Kendall, C., Shepherd, N., Crow, P. & Barr, H. Near-infrared Raman spectroscopy for the classification of epithelial pre-cancers and cancers. *Journal of Raman Spectroscopy* **33**, 564-573 (2002).
21. Shafer-Peltier, K. E. et al. Raman microspectroscopic model of human breast tissue: implications for breast cancer diagnosis in vivo. *Journal of Raman Spectroscopy* **33**, 552-563 (2002).
22. Nijssen, A. et al. Discriminating basal cell carcinoma from its surrounding tissue by Raman spectroscopy. *Journal of Investigative Dermatology* **119**, 64-69 (2002).
23. Utzinger, U. et al. Near-infrared Raman spectroscopy for in vivo detection of cervical precancers. *Applied Spectroscopy* **55**, 955-959 (2001).
24. Kaminaka, S., Yamazaki, H., Ito, T., Kohda, E. & Hamaguchi, H. O. Near-infrared Raman spectroscopy of human lung tissues: possibility of molecular-level cancer diagnosis. *Journal of Raman Spectroscopy* **32**, 139-141 (2001).
25. Schut, T. C. B. et al. In vivo detection of dysplastic tissue by Raman spectroscopy. *Analytical Chemistry* **72**, 6010-6018 (2000).

26. Gniadecka, M., Wulf, H. C., Mortensen, N. N., Nielsen, O. F. & Christensen, D. H. Diagnosis of basal cell carcinoma by Raman spectroscopy. *Journal of Raman Spectroscopy* **28**, 125-129 (1997).
27. Frank, C. J., Redd, D. C. B., Gansler, T. S. & Mccreery, R. L. Characterization of Human Breast Biopsy Specimens with near-Ir Raman-Spectroscopy. *Analytical Chemistry* **66**, 319-326 (1994).
28. Min, Y. K., Yamamoto, T., Kohda, E., Ito, T. & Hamaguchi, H. 1064 nm near-infrared multichannel Raman spectroscopy of fresh human lung tissues. *Journal of Raman Spectroscopy* **36**, 73-76 (2005).
29. Notingher, I., Jell, G., Lohbauer, U., Salih, V. & Hench, L. L. In situ non-invasive spectral discrimination between bone cell phenotypes used in tissue engineering. *Journal of Cellular Biochemistry* **92**, 1180-1192 (2004).
30. Krafft, C., Knetschke, T., Siegner, A., Funk, R. H. W. & Salzer, R. Mapping of single cells by near infrared Raman microspectroscopy. *Vibrational Spectroscopy* **32**, 75-83 (2003).
31. Omberg, K. M. et al. Raman spectroscopy and factor analysis of tumorigenic and non-tumorigenic cells. *Applied Spectroscopy* **56**, 813-819 (2002).
32. Ashkin, A., Dziedzic, J. M., Bjorkholm, J. E. & Chu, S. Observation of a Single-Beam Gradient Force Optical Trap for Dielectric Particles. *Optics Letters* **11**, 288-290 (1986).
33. Ashkin, A. & Dziedzic, J. M. Optical Trapping and Manipulation of Viruses and Bacteria. *Science* **235**, 1517-1520 (1987).
34. Ashkin, A., Dziedzic, J. M. & Yamane, T. Optical Trapping and Manipulation of Single Cells Using Infrared-Laser Beams. *Nature* **330**, 769-771 (1987).
35. Bustamante, C., Bryant, Z. & Smith, S. B. Ten years of tension: single-molecule DNA mechanics. *Nature* **421**, 423-427 (2003).
36. Visscher, K., Schnitzer, M. J. & Block, S. M. Single kinesin molecules studied with a molecular force clamp. *Nature* **400**, 184-189 (1999).
37. Molloy, J. E. & Padgett, M. J. Lights, action: optical tweezers [Review]. *Contemporary Physics* **43**, 241-258 (2002).
38. Xie, C. G., Dinno, M. A. & Li, Y. Q. Near-infrared Raman spectroscopy of single optically trapped biological cells. *Optics Letters* **27**, 249-251 (2002).
39. Xie, C. G. & Li, Y. Q. Cohfocal micro-Raman spectroscopy of single biological cells using optical trapping and shifted excitation difference techniques. *Journal of Applied Physics* **93**, 2982-2986 (2003).
40. Chan, J. W. et al. Reagentless identification of single bacterial spores in aqueous solution by confocal laser tweezers Raman spectroscopy. *Analytical Chemistry* **76**, 599-603 (2004).
41. Xie, C. G., Goodman, C., Dinno, M. A. & Li, Y. Q. Real-time Raman spectroscopy of optically trapped living cells and organelles. *Optics Express* **12**, 6208-6214 (2004).
42. Mannie, M. D., McConnell, T. J., Xie, C. G. & Li, Y. Q. Activation-dependent phases of T cells distinguished by use of optical tweezers and near infrared Raman spectroscopy. *Journal of Immunological Methods* **297**, 53-60 (2005).
43. Xie, C. G., Li, Y. Q., Tang, W. & Newton, R. J. Study of dynamical process of heat denaturation in optically trapped single microorganisms by near-infrared Raman spectroscopy. *Journal of Applied Physics* **94**, 6138-6142 (2003).
44. Ajito, K., Han, C. X. & Torimitsu, K. Detection of glutamate in optically trapped single nerve terminals by Raman spectroscopy. *Analytical Chemistry* **76**, 2506-2510 (2004).
45. Deng, J. L., Wei, Q., Zhang, M. H., Wang, Y. Z. & Li, Y. Q. Study of the effect of alcohol on single human red blood cells using near-infrared laser tweezers Raman spectroscopy. *Journal of Raman Spectroscopy* **36**, 257-261 (2005).

46. Chan, J. W. et al. Micro-Raman spectroscopy detects individual neoplastic and normal hematopoietic cells. *Biophysical Journal* **90**, 648-656 (2006).
47. Chan, J. W. et al. Non-destructive identification of individual leukemia cells by laser trapping Raman spectroscopy. *Analytical Chemistry* **80** 2180-2187 (2008)
48. Uzunbajakava, N., Lenferink, A., Krann, Y., Willekens, B., Vrensen, G., Greve, J., Otto, C. *Biopolymers* 72, 1-9 (2003)
49. Notingher, I., Jell, G., Lohbauer, U., Salih, V., and Hench, L. L. *Journal of Cellular Biochemistry* 2004, *92,* 1180-1192.
50. Mannie, M. D., McConnell, T. J., Xie, C. G., and Li, Y. Q. *Journal of Immunological Methods* 2005, *297,* 53-60.
51. Chan, J. W., Taylor, D. S., Thompson, D. L. The effect of cell fixation on the discrimination of normal and leukemia cells with laser tweezers Raman spectroscopy. *Biopolymers* **91**, 132-139 (2009)
52. Lau, A. Y., Lee, L. P., Chan, J. W., An integrated optofluidic platform for Raman activated cell sorting. *Lab Chip* **8**, 1116-1120 (2008)
53. Yamada, M., Nakashima, M., Seki M. Pinched flow fractionation: continuous size separation of particles utilizing a laminar flow profile in a pinched microchannel. *Analytical Chemistry* **76**, 5465-5471 (2004)